Click Here for Full Article

Evidence for a major change in silicon cycling in the subarctic North Pacific at 2.73 Ma

B. C. Reynolds,[1] M. Frank,[2] and A. N. Halliday[3]

[1]   The initiation of Northern Hemisphere glaciation in the subarctic North Pacific at ~2.73 Ma was marked by an abrupt cessation of high opaline accumulation, considered to result from an increased stratification of the water column that should have led to higher utilization of nutrients in the surface ocean. We present a new stable Si isotope-based record of Si utilization that is hard to reconcile with this model. A drop in ^{30}Si/^{28}Si by 0.4‰ at 2.73 Ma is coincident with an increase in bulk N isotope composition. The contrasting utilization records cannot have been both caused by a hydrographic change alone. Excluding a change in the Si:N export ratio, these results either imply a relative increase in silicic acid supplied to the surface waters or a change in its Si isotope composition. While it is impossible to distinguish between these two possibilities, both imply a regional or global change in the Si biogeochemical cycle, potentially caused by an enhanced storage of Si in the underlying deep waters of the Pacific.

Citation: Reynolds, B. C., M. Frank, and A. N. Halliday (2008), Evidence for a major change in silicon cycling in the subarctic North Pacific at 2.73 Ma, *Paleoceanography*, *23*, PA4219, doi:10.1029/2007PA001563.

1.   Introduction

[2]   The major intensification of Northern Hemisphere Glaciation (NHG) and the associated growth of continental ice sheets occurred in the late Pliocene. It is recorded globally by a pronounced change toward heavier oxygen isotopic compositions of benthic foraminifera, markedly increased glacial/interglacial amplitudes of ice volume and temperature [*Raymo*, 1994; *Lisiecki and Raymo*, 2005] and the onset of significant occurrences of ice-rafted debris (IRD) in high-latitude sediments [*Shackleton et al.*, 1984; *Rea and Schrader*, 1985; *Maslin et al.*, 1995; *Murphy et al.*, 2002]. In the subarctic North Pacific this transition and the start of IRD deposition were marked by an abrupt decrease in abundance and accumulation of biogenic opal, mainly in the form of diatoms, at 2.73 Ma [*Rea and Schrader*, 1985; *Maslin et al.*, 1995; *Tiedemann and Haug*, 1995; *Haug et al.*, 1999]. Prior to this time, high opal mass accumulation rates (Opal MAR > 2 g cm^{-2} ka^{-1}) were sustained by enhanced upwelling rates of nutrient rich deep waters into the surface oceans, indicating a lack of water column stratification. In contrast, in the modern subarctic Pacific a strong halocline prevents vertical mixing and isolates the euphotic zone from deeper waters [*Warren*, 1983; *Emile-Geay et al.*, 2003]. It is not known if the proposed stratification in the subarctic North Pacific was only a regional phenomenon or if it was part of a global reorganization related to gradual cooling [see *Cortese et al.*,

2004]. For example, a similar drop in opal accumulation was also found at approximately the same time in ODP cores 885, 886 and 887 across the subarctic North Pacific shortly before the Matayama/Gauss boundary [*Rea and Snoeckx*, 1995; *Snoeckx et al.*, 1995], and marks the end of a long period of enhanced opal accumulation that had lasted since ~8 Ma (termed the "Biogenic Bloom" [*Farrell et al.*, 1995]). Stable nitrogen and silicon isotopes can be used as proxies for nutrient utilization in order to assess the importance of changes in nutrient dynamics for the decrease in biogenic sedimentation.

[3]   In the modern high-latitude North Pacific, spring blooms of diatoms partially utilize the abundant nutrients [*Tsuda et al.*, 2005], but iron limitation results in year-round high-nutrient but low-chlorophyll concentrations in the surface waters (HNLC) [*Martin and Fitzwater*, 1988]. The biological utilization of nutrients causes mass-dependent isotope fractionation, with the lighter isotopes being preferentially incorporated into the diatoms' organic matter and frustules during biomineralization. This can be observed in the stable isotope ratios of C (^{13}C/^{12}C), N (^{15}N/^{14}N) and Si (^{30}Si/^{28}Si) [*Tieszen*, 1978; *Altabet and Francois*, 1994; *De La Rocha et al.*, 1997], which are expressed in δ notation as relative deviations from a standard in parts per thousand [*Coplen et al.*, 2002], e.g., δ^{13}C, δ^{15}N and δ^{30}Si. Despite the importance of Si, only three published studies have so far used Si stable isotopes as proxies for understanding variations in past diatom productivity, or more exactly Si utilization [*De La Rocha et al.*, 1998; *Brzezinski et al.*, 2002; *Beucher et al.*, 2007]. However, we must also consider that changes in the marine Si isotope distribution might affect this Si utilization proxy. The records of Si utilization in the Southern Ocean show that during glacial periods δ^{30}Si values were significantly lower, which was related to lower Si utilization south of the modern Polar Front [*De La Rocha et al.*, 1998].

[1]Institute of Isotope Geochemistry and Mineral Resources, ETH Zurich, Zurich, Switzerland.
[2]Leibniz Institute of Marine Sciences at University of Kiel (IFM-GEOMAR), Kiel, Germany.
[3]Department of Earth Sciences, Oxford University, Oxford, UK.
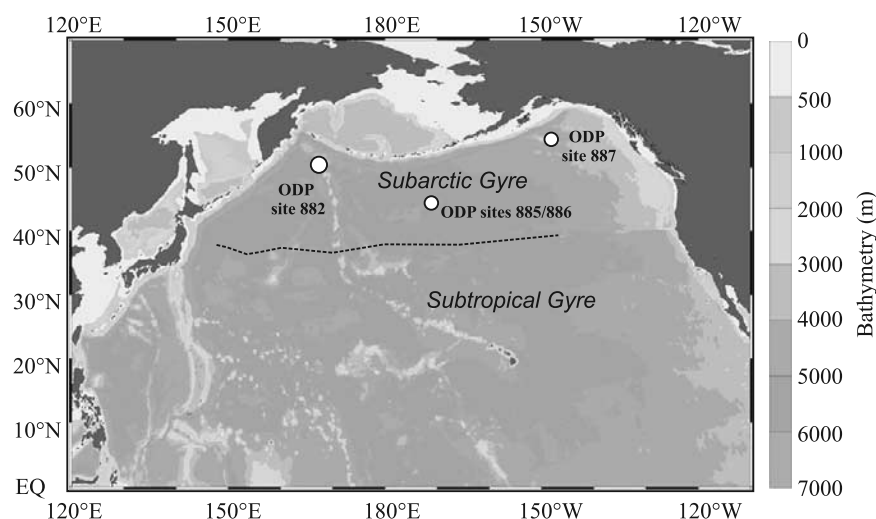
Figure 1. Map of the North Pacific showing the location of ODP core 882.

[4] We have investigated the biogenic opal deposited at ODP Site 882 for the period around 2.73 Ma marking a dramatic drop in opal MAR and the initiation of Northern Hemisphere Glaciation in the North Pacific [*Maslin et al.*, 1996; *Haug et al.*, 1999]. The bulk $\delta^{15}N$ composition of the opaline sediments of ODP core 882 from the western North Pacific (50° 21′N, 167° 35′E, and water depth 3,244 m) shows a marked increase that occurred contemporaneously with a drop in opal accumulation [*Sigman et al.*, 2004]. The results presented here provide the oldest paleoceanographic record of Si utilization and the first diatom Si isotope record outside the Southern Ocean. We show that Si utilization does not covary as expected with N utilization; the isotopic compositions actually inversely correlated. This correlation may indicate that both proxies reflect changes in the Si:N ratio of upwelling deep water rather than changes of the utilization in the surface waters alone.

2. Materials and Methods

[5] We have investigated the biogenic opal deposited at ODP Site 882 for the section between 106 and 116 m depth below surface, representing the period between 2.78 and 2.61 Ma (Figure 1), which includes the abrupt and irreversible drop in the biogenic opal content of the sediments [*Maslin et al.*, 1996; *Haug et al.*, 1999]. The chronology of the core is based on an astronomically calibrated stratigraphy for the past 4 Ma based on fine tuning the GRAPE density oscillations in the precession band to the summer insolation at 65°N (see *Tiedemann and Haug* [1995] for more details). The Gauss/Matuyama magnetic reversal is at 105.94 m in the composite core depth (mcd), or 2.61 Ma on the orbital time scale [*Deino et al.*, 2006]. The abrupt drop in the percentage of opal in the sediment core corresponds to an age of 2.73 Ma, which we will use in the discussion, even though this absolute age is not very well constrained. A down-core $\delta^{30}Si$ record was obtained from biogenic opal using high-resolution multiple-collector inductively coupled plasma mass spectrometry (MC-ICPMS), following a novel chromatographic separation and purification method of Si [*Georg et al.*, 2006b]. This new approach for Si isotope analyses has been shown to provide a better precision and sensitivity for water samples [*Georg et al.*, 2006b; *Reynolds et al.*, 2006a, 2006b] and is applied here to biogenic silica for the first time.

[6] Aggressive cleaning of the diatom frustules in order to remove trace metals for the analysis of biogenic opal is not required for the determination of Si isotope variations using the methods described here. Selected diatom samples showed excellent preservation under the SEM (Figure 2) and essentially no clay contamination. Tests demonstrated that contamination from clays (with Al/Si ~1) represents less than 1% of the total Si, following published procedures [*Shemesh et al.*, 1988]. Even if this trace amount of clay contributed $\delta^{30}Si$ values as low as −1‰, the measured $\delta^{30}Si$ value would only be shifted by 0.04‰, which is negligible and within the analytical uncertainty.

[7] A small amount of biogenic opal (0.5 mg) was transferred into a Teflon vial, dried down, and was then treated with concentrated perchloric acid which was evaporated at ~180°C. While still hot, the silicate was dissolved in 100 μl of 1 M NaOH, left overnight and then diluted to 5 ml with 0.01 M HCl. Acid cleaning of the opal was not essential since results with and without cleaning were indistinguishable, but the hot cleaning aided the dissolution under hot alkaline conditions. A sample aliquot was used to determine the Si concentration of the solutions (typically 50 ppm) using a colorimetric method on a spectrophotometer. An aliquot (typically 0.1 ml) of the stock solution was then loaded onto a precleaned 1.8 ml DOWEX 50W-X12 cation exchange resin bed (in H^+ form) and eluted with 5 ml of purified water (Milli-Q element 18.4 $M\Omega.cm^{-1}$). The resin had been precleaned with several rinses of HCl, HNO_3, and water, as well as a final wash with water ensuring neutral pH of the elute prior to loading. This technique utilizes the fact that Si will remain a neutral or negatively charged species above pH 2 and will not adsorb to the cation resin, while all cation species (pre-
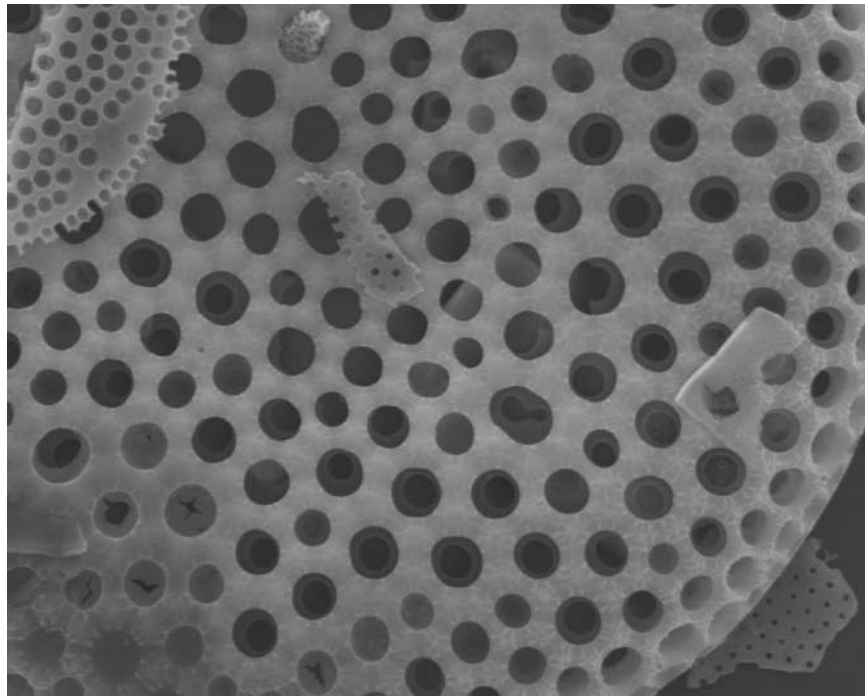
Figure 2. SEM photograph of a 2.63 Ma old diatom frustule sampled from 106.65 mbsf in ODP core 882.

dominantly Na, but also trace amounts of Al, Mg, etc.) will quantitatively adsorb and thus be fully removed from the analyte.

[8] The eluted solution was then diluted to 0.6 ppm Si in 0.002 N HCl for introduction into the NuPlasma 1700 high-resolution MC-ICPMS at ETH Zürich. The NuPlasma 1700 is unique in being able to achieve complete resolution of the three Si ion beams from all polyatomic isobaric interferences from the plasma source, including $^{14}N^{16}O^{+}$. The Si solutions and standards were introduced into the plasma via a Nu Instruments DSN desolvator equipped with a PFA nebulizer at a $60-80$ μl/min uptake rate. Background levels are reduced to 10^{-13} A for $^{28}Si^{+}$ by the use of a semi-demountable alumina-injector torch. The three Si ion beams were collected simultaneously on Faraday collectors, with typical intensities of 6×10^{-11} A for $^{28}Si^{+}$. Measurement protocols utilized standard-sample-standard bracketing. All results in this study were calculated using the $\delta^{30}Si$ notation for deviations of the measured $^{30}Si/^{28}Si$ from the international Si standard NBS28 in parts per thousand (‰). The long-term reproducibility was better than 0.14‰ $\delta^{30}Si$ (2 standard deviations of the mean) [*Reynolds et al.*, 2006b], and 6 duplicate samples processed through chemistry gave a better reproducibility than this (0.11‰ 2 s.d., n = 18). Samples were measured at least 5 times, which resulted in a 95% confidence level below 0.08‰ $\delta^{30}Si$, limited by our external reproducibility rather than the analytical error on the sample.

3. Results

[9] The theoretical relationship between the degree of nutrient utilization (f = relative decrease in N or Si concentration) and recorded stable isotope composition ($\delta^{15}N$ or

$\delta^{30}Si$) is shown on Figure 3, and can be described as follows, assuming either a Rayleigh-type model or a steady state model, respectively:

$$\text{Rayleigh}: \left(\delta^{15}N\right)_{AOpal} = \left(\delta^{15}N\right)_{iSW}$$
$$+ \left(\frac{1-f_N}{f_N}\right)\varepsilon_N \ln(1-f_N) \quad \text{or}$$
$$\text{steady state}: \left(\delta^{15}N\right)_{AOpal} = \left(\delta^{15}N\right)_{iSW}+\varepsilon_N(1-f_N)$$
$$\text{Rayleigh}: \left(\delta^{30}Si\right)_{AOpal} = \left(\delta^{30}Si\right)_{iSW}$$
$$+ \left(\frac{1-f_{Si}}{f_{Si}}\right)\varepsilon_{Si} \ln(1-f_{Si}) \quad \text{or}$$
$$\text{steady state}: \left(\delta^{30}Si\right)_{AOpal} = \left(\delta^{30}Si\right)_{iSW}+\varepsilon_{Si}(1-f_{Si})$$

where ε is the fractionation factor between seawater and biogenic opal for Si ($\varepsilon_{Si} \approx -1.1$) or N ($\varepsilon_N \approx -6$), and the subscripts *AOpal* and *iSW* refer to the accumulated biogenic opal composition and initial seawater composition, respectively. A steady state model assumes constant supply and export at equilibrium, while the Rayleigh-type model assumes a fixed input followed by fractional loss or export (in time or space). Results obtained from culture studies have not shown any species or temperature dependence of the Si isotope fractionation factor, which is $\varepsilon_{Si} \approx -1.1$‰ [*De La Rocha et al.*, 1997]. This degree of mass fractionation has been confirmed by seawater modeling [*Cardinal et al.*, 2005; *Reynolds et al.*, 2006a], but fractionation into in situ formed biogenic opal appears to be somewhat larger, up to $\varepsilon_{Si} \approx -1.6$‰ [*Varela et al.*, 2004; *Cardinal et al.*, 2007]. For any one type of model used,
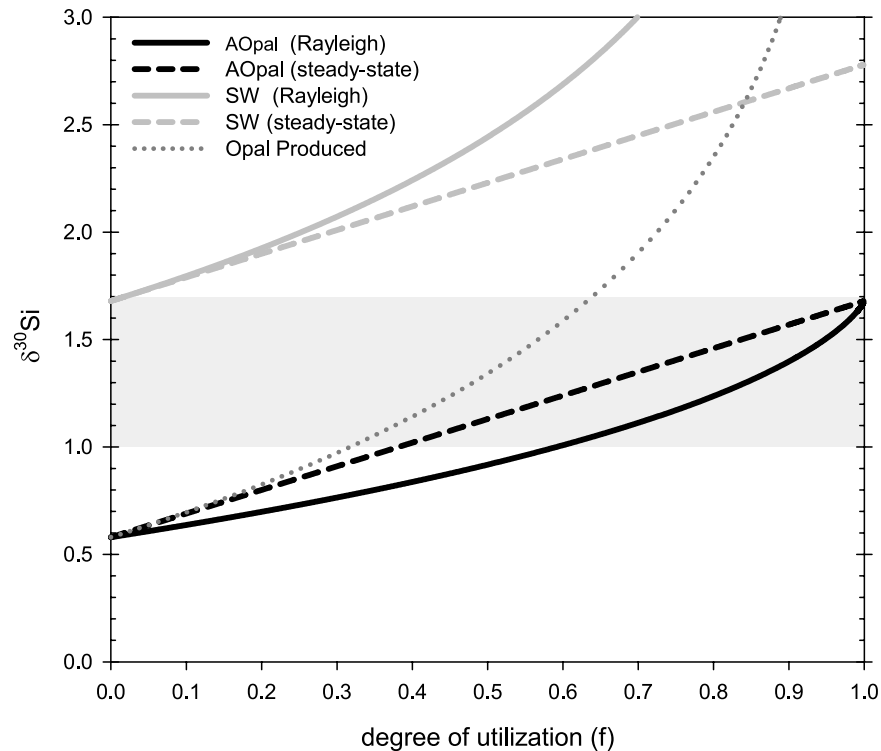
Figure 3. Theoretical changes in δ^{30}Si values of seawater (gray lines) and accumulated biogenic opal (black lines) as a function of the fraction of Si removed from seawater with an initial δ^{30}Si value of +1.7‰. Precipitation of opal follows either a Rayleigh-type fractionation model (solid lines) or a steady state system (dashed lines) behavior, with a fractionation factor of −1.1‰. The instantaneous composition of the diatoms growing under a Rayleigh-type fractionation model is also plotted (dotted line). The shaded area marks the range of observed δ^{30}Si values between +1.0 and +1.7‰.

there is only one other parameter relating the isotopic composition of the opal (δ^{30}Si) and the degree of utilization (*f*); the initial seawater composition. The initial isotope composition of the seawater is that supplied to the euphotic zone via upwelling (since atmospheric inputs of Si including dust dissolution are negligible).

[10] The results of the Si and N isotope composition of the diatom samples are shown in Figure 4 together with the opal accumulation in the sediment. The total observed range from +1.0 to +1.7‰ in δ^{30}Si (or +0.5 to +0.8‰ δ^{29}Si) is comparable to the amplitude measured over glacial-interglacial time scales in the Southern Ocean [*De La Rocha et al.*, 1998; *Brzezinski et al.*, 2002] and corresponds to almost 10 times the analytical uncertainty. Both the Si and N isotope compositions change exactly at the abrupt drop in percentage of opal in the sediment. When high opal accumulation rates prevailed, the δ^{30}Si values were consistently above +1.5‰, whereas after the 2.73 Ma transition the values consistently remained below +1.5‰. The striking result of a change by over 0.25‰ over a period of only about 5 ka has been duplicated, including sample reprocessing, and must reflect the composition of bulk diatomaceous opal in the sediment. However, after the major drop in the opal accumulation, relatively large fluctuations in the δ^{30}Si and δ^{15}N occurred, which were accompanied by an almost complete return to pretransition values just after

2.72 Ma, which also coincided with a small increase in opal accumulation. This may either indicate a brief rebound in the Si and N biogeochemistry after the major change at 2.73 Ma or the change was actually more gradual, despite the fact that low opal accumulation rates and low δ^{30}Si values became the normal state during the glacial-interglacial periods after 2.73 Ma. The record of bulk sediment δ^{15}N values [*Sigman et al.*, 2004] shows a marked gradual increase across the 2.73 Ma transition, with values below +3.5‰ prior to this event, and values consistently above 3‰ afterward. There is a clear inverse relationship between bulk sedimentary δ^{15}N and diatom δ^{30}Si values, as shown in Figure 5, with slopes of −3.2 (R^2 = 0.98). If Si and N utilization were to covary solely because of diatom productivity a positive slope of +5 would be expected, given a N isotope fractionation factor of ∼5–6‰ [*Sigman et al.*, 1999; *Altabet and Francois*, 2001; *Lourey et al.*, 2003].

[11] The abrupt change of >0.3‰ in δ^{30}Si at 2.73 Ma is relatively large compared to the isotopic fractionation factor (ε_{Si}) occurring during biogenic opal production by diatoms [*De La Rocha et al.*, 1997], which was estimated at −1.1‰ δ^{30}Si. Assuming that all recorded δ^{30}Si variations are solely a function of Si utilization in the surface oceans, we can model the apparent utilization as shown in Figure 3, assuming that the highest recorded δ^{30}Si value occurred when there was complete utilization of the available Si.
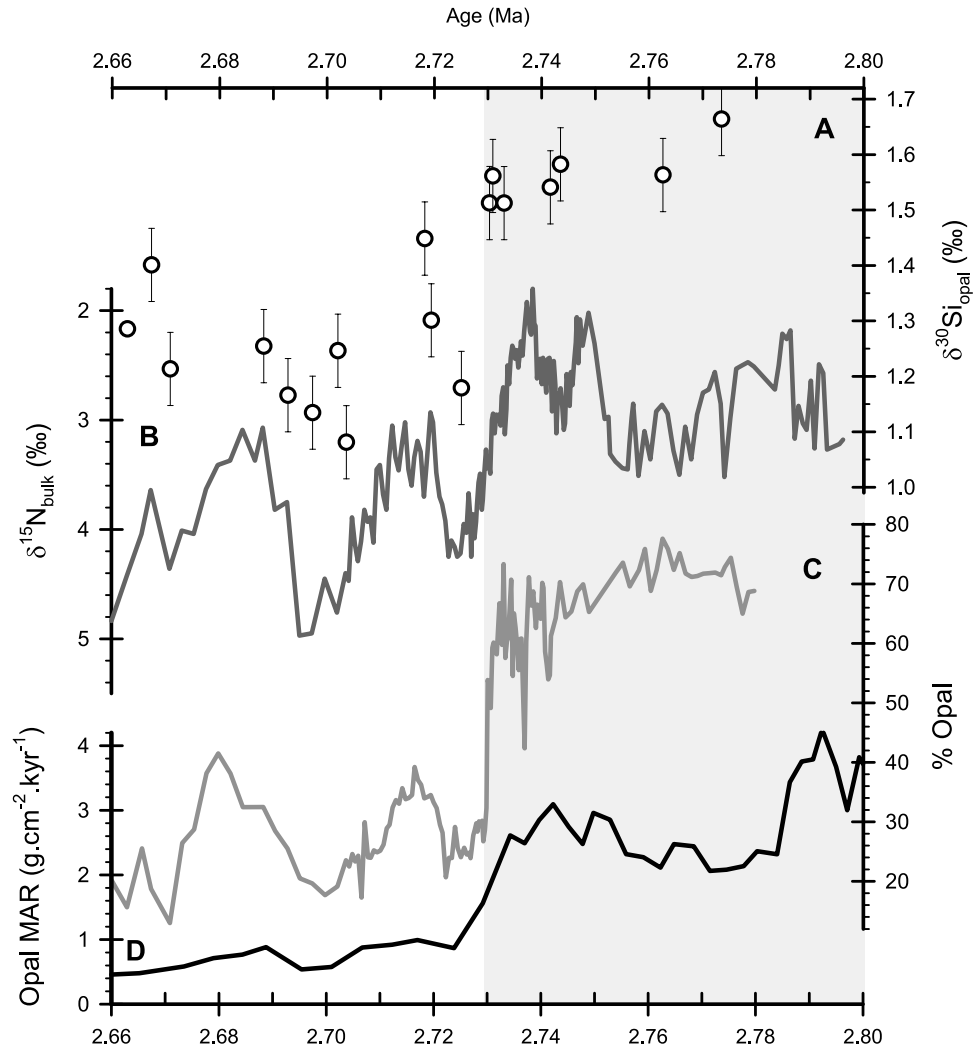
Figure 4. Comparison of the records for the time period from 2.66 to 2.8 Ma from ODP core 882 (a) diatom δ^{30}Si values, (b) bulk sediment δ^{15}N, (c) percentage of opal in the sediment, and (d) opal mass accumulation rates (MAR).

With complete utilization the δ^{30}Si value of the opal export is equal to the dissolved δ^{30}Si of the source waters (+1.7‰). The lowest δ^{30}Si value corresponds to either 40% or 60% Si utilization, based upon a steady state or Rayleigh-type fractionation model, respectively. The abrupt change at 2.73 Ma is equivalent to a 33% and 18% drop in utilization, on the basis of the same respective models. However, it could equally be argued that upon stratification, the more suitable model changed from a steady state (continuous upwelling) to a Rayleigh-type (seasonally stratified) model, and thus the change in δ^{30}Si from 1.5‰ to 1.2‰ may represent a change in utilization of as little as 8%. Although the δ^{30}Si values give a sense of change in the utilization, they cannot uniquely quantify the actual degree of utilization.

4. Discussion

[12] As already stated, the abrupt decrease in biogenic opal accumulation in ODP core 882 at 2.73 Ma has been interpreted as the result of a reduction in the supply of nutrients to the surface waters [*Rea et al.*, 1993; *Haug et al.*, 1999, 2005; *Sigman et al.*, 2004]. This drop in nutrient supply is thought to have been caused by a stratification of the water column leading to a concomitant reduction in mixing of deeper waters into the surface layer [*Haug et al.*, 1999]. Modern diatom productivity could not increase by more than 30% before being stopped by the complete removal of Si from the summer time surface layer [*Andreev et al.*, 2002]. As productivity indicated by the opal MAR was over 200% higher prior to 2.73 Ma, the observed changes cannot have been the result of a higher consumption of the same supply rate of major nutrients [*Sigman et al.*, 2004], which means that active upwelling must have occurred prior to 2.73 Ma. However, processes that drove this abrupt stratification and its implications for the global climate are not well constrained. The increase in bulk sediment δ^{15}N values was attributed to a more complete consumption of surface nitrate by phytoplankton linked to
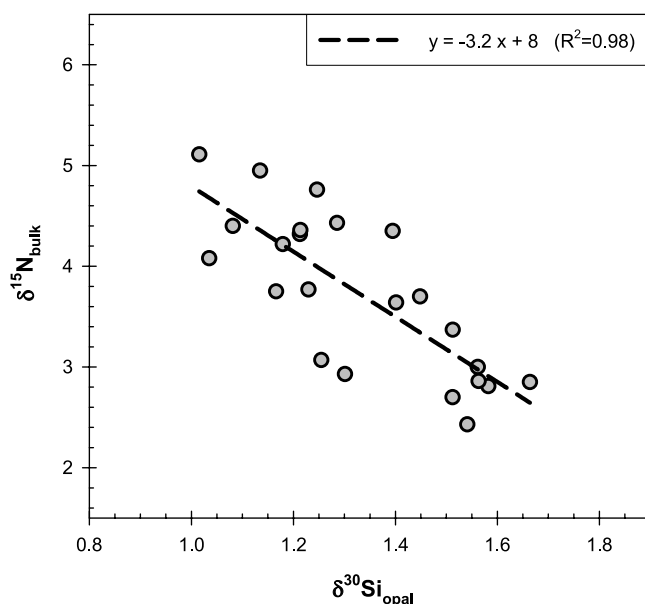
Figure 5. The published bulk sediment δ^{15}N versus diatom δ^{30}Si obtained in this study. Regression line represents the correlation ($R^2 = 0.98$) that is significant at the 97% level.

stratification due to lower supply of nitrate into the surface layer [*Haug et al.*, 1999; *Sigman et al.*, 2004]. A reduced opal production without a reduction in nitrate supply would lead to less N utilization and thus lower δ^{15}N values.

[13] Theoretically, Si isotopes should behave the same as N isotopes, with stratification leading to a reduction in Si supply and a correspondingly greater degree of Si utilization resulting in higher δ^{30}Si values. However, the main increase in δ^{15}N as well as shorter-term changes, are strongly inversely correlated with the δ^{30}Si variations (Figure 5). In summary, the two proxies provide opposing results on nutrient utilization before and after 2.73 Ma. The central question of this study is therefore how the contrasting stable N and Si isotope variations can be reconciled.

[14] We will first reconsider the inherent potential problems in the opal-based isotope record. While potential reasons for stable Si or N isotope variations other than changes in nutrient utilization can be found, as extensively reviewed by *De La Rocha* [2006], they would not explain the negative correlation between these two isotope systems. This correlation most likely reflects changes in the relative utilization of N compared to Si, and thus a change in the upwelling and/or export ratio of Si:N, which will be considered separately. However, we must also consider changes in the marine Si isotope distribution affecting the Si utilization proxy.

4.1. Potential Difficulties in the Si Isotope Record

[15] Silicon isotopes should be comparatively robust to diagenetic alteration given the mass balance within the sediment column. The excellent preservation shown in Figure 2 provides powerful evidence against significant partial dissolution within the sediment. However, dissolu-

tion of biogenic opal prior to burial in the sediment is substantial. In the water column and at the sediment-water interface >95% of the opal exported from the surface oceans is dissolved [*Treguer et al.*, 1995]. Thus the degree to which recorded δ^{30}Si values reflect the average δ^{30}Si values of the opal produced in the surface layer is not well constrained, and there will be a bias in the sediment record toward diatom frustules that are less prone to dissolution. Dissolution has been shown to alter the diatom species assemblage in marine cores [*Shemesh et al.*, 1989; *Mohan et al.*, 2006]. As the opal δ^{30}Si values do not appear to be species-dependent, the loss of any one species should not affect the recorded δ^{30}Si value per se, but only the degree to which the sedimentary opal reflects the average annual Si utilization. Diatom species assemblages or dissolution rates may well change over the seasonal cycle, and thus the δ^{30}Si record will be affected and will not record average annual δ^{30}Si values of opal export. However, given that the species assemblages in the core do not strongly vary before and after the transition [*Swann et al.*, 2006], the relative δ^{30}Si variations within the core should not be greatly affected by dissolution. Clearly more work is required to assess the validity of δ^{30}Si records for recording variations in Si utilization of surface waters but there is no evidence that the isotopic variations reflect changes in dissolution.

4.2. Relative Changes in Si and N Export

[16] A similar inverse relationship between δ^{30}Si and δ^{15}N values has been observed on glacial-interglacial time scales for the other existing Late Quaternary δ^{30}Si records from the Southern Ocean [*De La Rocha et al.*, 1998; *Brzezinski et al.*, 2002]. This observation led to the development of the "silica leakage hypothesis," which relates the global N and Si biogeochemical cycles to the enhanced drawdown of atmospheric carbon dioxide during glacial periods through the availability of Fe in the Southern Ocean [*Brzezinski et al.*, 2002; *Matsumoto et al.*, 2002]. It was shown that the uptake of Si and N by diatoms can be altered by the availability of Fe [*Hutchins and Bruland*, 1998]. Thus changes in Fe availability could be a potential mechanism to explain the contrasting behavior of Si and N isotopes and the corresponding inferred utilization [*Brzezinski et al.*, 2002; *Matsumoto et al.*, 2002]. A shift to Fe-limiting conditions during interglacials causes high Si:N uptake ratios (>4:1, compared with 1:1 under Fe-replete conditions), higher Si uptake (for the same overall productivity), and thus higher δ^{30}Si values and lower δ^{15}N values. The observed shifts shown in Figure 6 in stable Si and N isotopes across the ~2.7 Ma onset of stratification could be interpreted in a similar way, invoking a change from Fe-limiting conditions to Fe-replete conditions for diatom productivity. However, there are two major problems with explaining the stable isotope variations in terms of a reduction in Fe-limiting conditions and Fe enriched waters after 2.73 Ma: first, opal productivity should have increased with Fe availability rather than decreased, as observed; second, stratification and evolution toward the modern North Pacific implies enhanced Fe depletion as observed today rather than the relief of Fe stress required to explain the stable isotope variations. We thus rule out potential
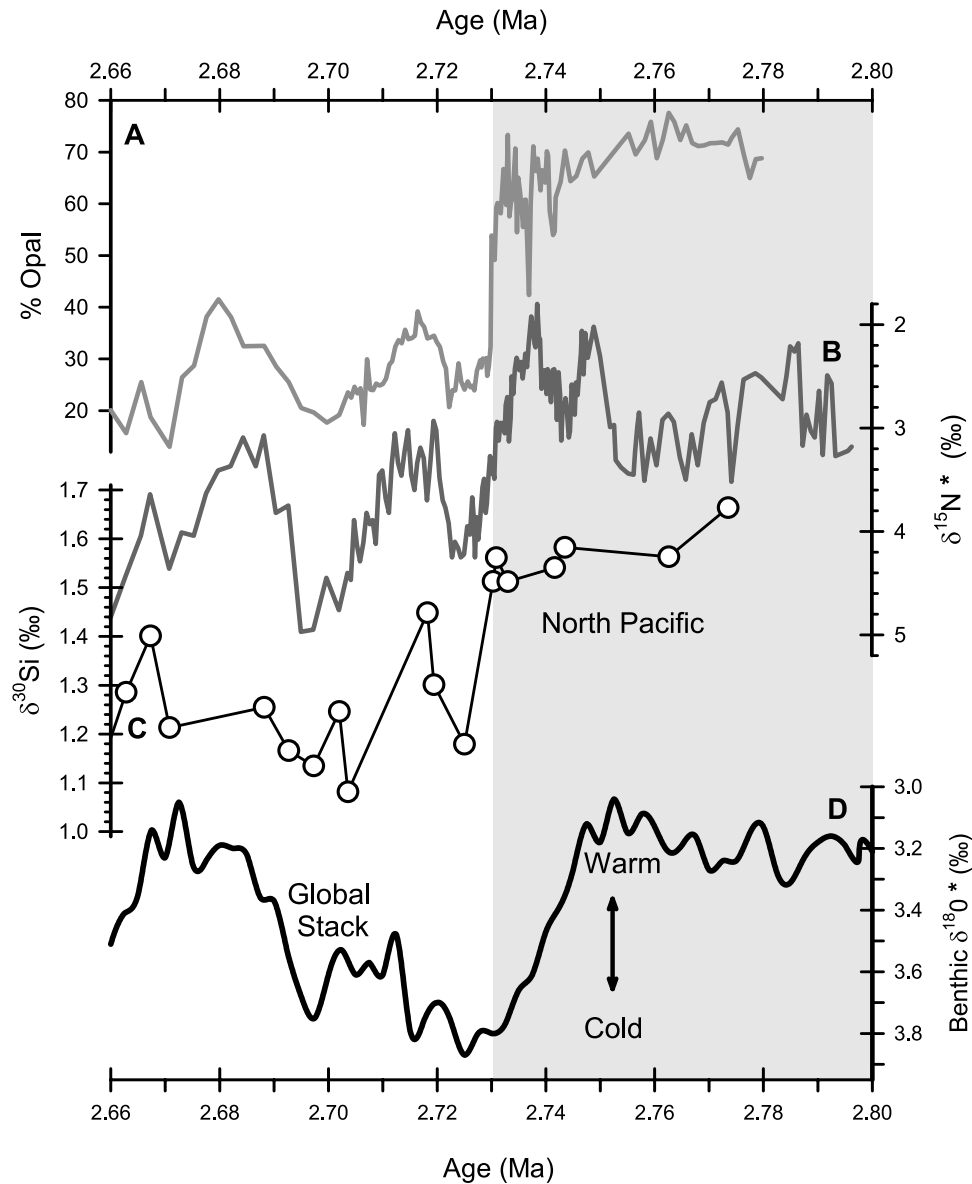
Figure 6. Comparison of records from (a–c) ODP core 882 to (d) the globally stacked benthic δ^{18}O values [*Lisiecki and Raymo*, 2005]. Figure 6a shows the percentage of opal in ODP core 882, Figure 6b shows bulk sedimentary δ^{15}N values (*NB inverted scale), and Figure 6c shows diatom δ^{30}Si values. The global δ^{18}O stack (inverted scale) reflects global ice volume and has been adjusted by +10 ka, to align the Matuyama/Gauss boundary to a glacial period at 2.61 Ma on the orbital time scale [*Deino et al.*, 2006].

effects of Fe fertilization as a cause for the observed negative correlation between N and Si stable isotope variations, despite the fact that dust input (and accompanying Fe supply) increased markedly in the late Pliocene, though significantly earlier than 2.73 Ma [*Rea et al.*, 1998].

[17] Another way to explain the apparent discrepancy between the stable isotope utilization proxies is to invoke productivity changes excluding diatom growth, thus decoupling N and Si utilization from each other. However, throughout the core, the phytoplankton community is dominated by essentially the same diatoms, just as the modern North Pacific productivity is today, and the species in the core do not strongly vary before and after the transition [*Swann et al.*,

2006]. There is no evidence for a change in nutrient utilization due to switching between siliceous and carbonate producing organisms, or the dominant diatom species, although we cannot rule out that possibility. If the utilization proxies are both correct, and the contrasting stable N and Si isotope variations are not due to changes in the relative export of Si and N, then they could be due to the relative import of Si and N into the surface waters from the deep sea, i.e., changing supply Si:N ratios.

4.3. Relative Changes in N and Si Supply

[18] The contrasting behavior of N and Si stable isotope variations across the period of time when enhanced strati-

fication of the North Pacific was established may have resulted from a change in the amount and composition of N and Si supplied to the surface waters. Thus changes in hydrography would be responsible, rather than changes in biological productivity alone, even though diatom productivity did decrease significantly. It is well known that the dissolved nutrient composition evolves from the deep Atlantic to the North Pacific where nutrient concentrations are highest, in particular those of Si (as reflected by high Si:N ratios) [*Ragueneau et al.*, 2000]. In order to explain the inversely correlated variations in $\delta^{15}N$ and $\delta^{30}Si$ values, we thus infer that the Si:N changed from low Si:N and more complete Si utilization (higher $\delta^{30}Si$ values) to conditions with high Si:N and more complete N utilization (higher $\delta^{15}N$ values). Nevertheless, changes in the isotope composition of the source waters may equally be inferred to explain the inverse correlation. The dissolved Si:N ratio of modern deep water in the North Pacific is extremely high but the source of this Si is poorly constrained. Some authors suggest that it is derived from the high opal productivity in the Southern Ocean [*Sarmiento et al.*, 2004], which separates the supply pathways of Si from those of N and P to the global and deep and intermediate ocean [*Dugdale and Wilkerson*, 2001; *Brzezinski et al.*, 2002]. However, other authors suggest that the Si is from within the North Pacific, either originating from release of Si from the Cascadia Basin in the NE Pacific [*Talley and Joyce*, 1992], or from crustal fluid venting from the easternmost Pacific plate [*Johnson et al.*, 2006]. Whatever the source of the dissolved Si is, we infer that lower Si:N ratio in waters upwelling in the North Pacific prior to 2.73 Ma may indicate the onset of the supply of Si from this source at this time (Figure 6).

4.4. Potential Changes in Marine $\delta^{30}Si$ Values

[19] The average seawater $\delta^{30}Si$ value may also vary over time because of isotopic changes in the global Si inputs to the oceans. The $\delta^{30}Si$ value adjusts to a new isotopic equilibrium where the Si isotopic inputs to the oceans are balanced primarily by their output in the form of biogenic opal. While it has been shown that the strength of the Si cycle has little effect on the mean $\delta^{30}Si$ value of seawater [*De La Rocha and Bickle*, 2005], the isotope composition of the inputs from the continents depends on weathering and the hydrological cycle, and these potentially can lead to differences on the order of $\sim$0.2‰ over time scales that are longer the than residence time of Si in the oceans (>15 ka [*Treguer et al.*, 1995]) [*Georg et al.*, 2006a]. The changes in the $\delta^{30}Si$ recorded at 2.73 Ma are clearly too large and too abrupt to be the result of changes in the terrestrial inputs to the oceans, requiring both an unrealistically abrupt change in continental $\delta^{30}Si$ inputs by more than 0.4‰, and a shorter oceanic residence time of Si. On the longer time scales of the whole record of this study, seawater $\delta^{30}Si$ values could change due redistribution of opal accumulation with changes in the opal $\delta^{30}Si$ removed from seawater into the sediments. It is not possible to prove unambiguously that seawater $\delta^{30}Si$ values remained constant over the time scale of the complete record presented here, but changes on time scales <10 ka must have been related to regional changes in Si utilization within the oceans.

[20] Modern deep water $\delta^{30}Si$ values range from +1.5‰ in the North Atlantic to +0.5‰ in North Pacific Deep Water [*De La Rocha et al.*, 2000; *Reynolds et al.*, 2006a]. This decrease in $\delta^{30}Si$ along the thermohaline conveyor is most likely the consequence of dissolution of diatoms with isotopically light biogenic Si. New modeling results indicate that the deep water $\delta^{30}Si$ gradient along the global conveyor should typically be about 0.3‰ (B. C. Reynolds, Modeling the modern marine $\delta^{30}Si$ distribution, submitted to *Global Biochemical Cycles*, 2008) and supports the low $\delta^{30}Si$ values of the North Pacific being anomalous. Available data so far indicate that intermediate water masses have more uniform Si isotope compositions between +1.3 and +1.6‰. It is these waters that supply the Si to the surface ocean (outside the Southern Ocean and Subpolar gyre of the North Pacific). Thus, for Si the initial isotope composition of surface waters that upwelled from deep waters is not uniform, but dependent upon geographical location and strength of the thermohaline circulation, as well as the mixing of deep and intermediate water masses. Unlike most of the rest of the surface oceans that are influenced by subantarctic mode water (which may have a more uniform $\delta^{30}Si$ composition), the North Pacific may be much more sensitive to changes in circulation. The modern North Pacific is an important exception to the typically low Si:N ratio in thermocline waters in that it shows high Si:N ratios ultimately derived from Si rich deep waters [*Sarmiento et al.*, 2004], which also have anomalously low $\delta^{30}Si$ values [*Reynolds et al.*, 2006a]. The inferred stratification of the North Pacific may have resulted in, or resulted from, changes in intermediate depth circulation which may easily have altered the $\delta^{30}Si$ values of the waters supplying Si to the surface ocean of the North Pacific. Hence variations in the opal $\delta^{30}Si$ values may not be related to any change in relative nutrient utilization as described above, but may have been a consequence of changes in the $\delta^{30}Si$ distribution with changes in ocean circulation. As the utilization model for the Pliocene record (Figure 3) required a source $\delta^{30}Si$ value of +1.7‰, but the modern composition of waters in the Pacific is less than this, the dissolved $\delta^{30}Si$ values of waters supplying the surface were probably different from those of the modern day. This could be due to a local change in the Si isotope signature composition of water masses, or, more likely, due to a different isotope balance of the global Si biogeochemical cycle, with a higher average $\delta^{30}Si$ value of seawater, or to a different distribution of marine $\delta^{30}Si$ values between the ocean basins.

5. Conclusions

[21] The onset of Northern Hemisphere Glaciation in the North Pacific was marked by a dramatic drop in the biogenic opal mass accumulation at 2.73 Ma, caused by a stratification of the surface layer of the ocean. Two independent proxies for nutrient utilization provide conflicting evidence: Si isotopes from diatom samples presented here became lighter indicating less efficient utilization, while N isotopes became heavier after 2.73 Ma indicating increased utilization. The inverse correlation between $\delta^{15}N$ and $\delta^{30}Si$ cannot be explained by local changes in productivity and

stratification alone. Prior to stratification, the high opal productivity was supported by vigorous upwelling of waters in the subarctic gyre of the North Pacific. After the onset of stratification, a reduced circulation and upwelling of deep waters with higher Si:N ratios are inferred to explain the reduced Si utilization, but at the same caused a more complete N utilization in the North Pacific. Inferred higher Si:N in the North Pacific after 2.73 Ma is supported by the high Si:N ratios observed in deep waters in the North Pacific but changes in the isotope composition of the source waters cannot be excluded as a cause for the observed Si isotope changes in the sedimentary record.

References

Altabet, M. A., and R. Francois (1994), Sedimentary nitrogen isotopic ratio as a recorder for surface ocean nitrate utilization, *Global Biogeochem. Cycles*, *8*(1), 103–116, doi:10.1029/93GB03396.

Altabet, M. A., and R. Francois (2001), Nitrogen isotope biogeochemistry of the Antarctic polar frontal zone at 170°W, *Deep Sea Res., Part II*, *48*(19–20), 4247–4273, doi:10.1016/S0967-0645(01)00088-1.

Andreev, A., M. Kusakabe, M. Honda, A. Murata, and C. Saito (2002), Vertical fluxes of nutrients and carbon through the halocline in the western subarctic Gyre calculated by mass balance, *Deep Sea Res., Part II*, *49*(24–25), 5577–5593, doi:10.1016/S0967-0645(02)00200-X.

Beucher, C. P., M. A. Brzezinski, and X. Crosta (2007), Silicic acid dynamics in the glacial sub-Antarctic: Implications for the silicic acid leakage hypothesis, *Global Biogeochem. Cycles*, *21*, GB3015, doi:10.1029/2006GB002746.

Brzezinski, M. A., C. J. Pride, V. M. Franck, D. M. Sigman, J. L. Sarmiento, K. Matsumoto, N. Gruber, G. H. Rau, and K. H. Coale (2002), A switch from $Si(OH)_4$ to NO_3^- depletion in the glacial Southern Ocean, *Geophys. Res. Lett.*, *29*(12), 1564, doi:10.1029/2001GL014349.

Cardinal, D., N. Savoye, T. W. Trull, L. Andre, E. E. Kopczynska, and F. Dehairs (2005), Variations of carbon remineralisation in the Southern Ocean illustrated by the Ba_{xs} proxy, *Deep Sea Res., Part I*, *52*(2), 355–370, doi:10.1016/j.dsr.2004.10.002.

Cardinal, D., N. Savoye, T. W. Trull, F. Dehairs, E. E. Kopczynska, F. Fripiat, J.-L. Tison, and L. Andre (2007), Silicon isotopes in spring Southern Ocean diatoms: Large zonal changes despite homogeneity among size fractions, *Mar. Chem.*, *106*(1–2), 46–62.

Coplen, T. B., et al. (2002), Isotope-abundance variations of selected elements (IUPAC technical report), *Pure Appl. Chem.*, *74*(10), 1987–2017, doi:10.1351/pac200274101987.

Cortese, G., R. Gersonde, C. D. Hillenbrand, and G. Kuhn (2004), Opal sedimentation shifts in the world ocean over the last 15 Myr, *Earth Planet. Sci. Lett.*, *224*(3–4), 509–527, doi:10.1016/j.epsl.2004.05.035.

Deino, A. L., J. D. Kingston, J. M. Glen, R. K. Edgar, and A. Hill (2006), Precessional forcing of lacustrine sedimentation in the late Cenozoic Chemeron Basin, Central Kenya Rift, and calibration of the Gauss/Matuyama boundary, *Earth Planet. Sci. Lett.*, *247*(1–2), 41–60, doi:10.1016/j.epsl.2006.04.009.

De La Rocha, C. L. (2006), Opal-based isotopic proxies of paleoenvironmental conditions, *Global Biogeochem. Cycles*, *20*, GB4S09, doi:10.1029/2005GB002664.

De La Rocha, C. L., and M. J. Bickle (2005), Sensitivity of silicon isotopes to whole-ocean changes in the silica cycle, *Mar. Geol.*, *217*(3–4), 267–282, doi:10.1016/j.margeo.2004.11.016.

De La Rocha, C. L., M. A. Brzezinski, and M. J. DeNiro (1997), Fractionation of silicon isotopes by marine diatoms during biogenic silica formation, *Geochim. Cosmochim. Acta*, *61*(23), 5051–5056, doi:10.1016/S0016-7037(97)00300-1.

De La Rocha, C. L., M. A. Brzezinski, M. J. DeNiro, and A. Shemesh (1998), Silicon-isotope composition of diatoms as an indicator of past oceanic change, *Nature*, *395*(6703), 680–683, doi:10.1038/27174.

De La Rocha, C. L., M. A. Brzezinski, and M. J. DeNiro (2000), A first look at the distribution of the stable isotopes of silicon in natural waters, *Geochim. Cosmochim. Acta*, *64*(14), 2467–2477, doi:10.1016/S0016-7037(00)00373-2.

Dugdale, R. C., and F. P. Wilkerson (2001), Sources and fates of silicon in the ocean: The role of diatoms in the climate and glacial cycles, *Sci. Mar.*, *65*, 141–152, doi:10.3989/scimar.2001.65s2141.

Emile-Geay, J., M. A. Cane, N. Naik, R. Seager, A. C. Clement, and A. van Geen (2003), Warren revisited: Atmospheric freshwater fluxes and "Why is no deep water formed in the North Pacific", *J. Geophys. Res.*, *108*(C6), 3178, doi:10.1029/2001JC001058.

Farrell, J. W., I. Raffi, T. R. Janecek, D. W. Murray, M. Levitan, K. A. Dadey, K.-C. Emeis, M. Lyle, J.-A. Flores, and S. Hovan (1995), Late Neogene sedimentation patterns in the eastern equatorial Pacific Ocean, *Proc. Ocean Drill. Program Sci. Results*, *138*, 717–756.

Georg, R. B., B. C. Reynolds, M. Frank, and A. N. Halliday (2006a), Mechanisms controlling the silicon isotopic compositions of river waters, *Earth Planet. Sci. Lett.*, *249*(3–4), 290–306, doi:10.1016/j.epsl.2006.07.006.

Georg, R. B., B. C. Reynolds, M. Frank, and A. N. Halliday (2006b), New sample preparation techniques for determination of Si isotope composition using MC-ICPMS, *Chem. Geol.*, *235*(1–2), 95–104, doi:10.1016/j.chemgeo.2006.06.006.

Haug, G. H., D. M. Sigman, R. Tiedemann, T. F. Pedersen, and M. Sarnthein (1999), Onset of permanent stratification in the subarctic Pacific Ocean, *Nature*, *401*(6755), 779–782, doi:10.1038/44550.

Haug, G. H., et al. (2005), North Pacific seasonality and the glaciation of North America 2.7 million years ago, *Nature*, *433*(7028), 821–825, doi:10.1038/nature03332.

Hutchins, D. A., and K. W. Bruland (1998), Iron-limited diatom growth and Si: N uptake ratios in a coastal upwelling regime, *Nature*, *393*(6685), 561–564, doi:10.1038/31203.

Johnson, H. P., S. L. Hautala, T. A. Bjorklund, and M. R. Zarnetske (2006), Quantifying the North Pacific silica plume, *Geochem. Geophys. Geosyst.*, *7*, Q05011, doi:10.1029/2005GC001065.

Lisiecki, L. E., and M. E. Raymo (2005), A Pliocene-Pleistocene stack of 57 globally distributed benthic $\delta^{18}O$ records, *Paleoceanography*, *20*, PA1003, doi:10.1029/2004PA001071.

Lourey, M. J., T. W. Trull, and D. M. Sigman (2003), Sensitivity of $\delta^{15}N$ of nitrate, surface suspended and deep sinking particulate nitrogen to seasonal nitrate depletion in the Southern Ocean, *Global Biogeochem. Cycles*, *17*(3), 1081, doi:10.1029/2002GB001973.

Martin, J. H., and S. E. Fitzwater (1988), Iron deficiency limits phytoplankton growth in the northeast Pacific subarctic, *Nature*, *331*(6154), 341–343, doi:10.1038/331341a0.

Maslin, M. A., G. H. Haug, M. Sarnthein, R. Tiedemann, H. Erlenkeuser, and R. Stax (1995), Northwest Pacific Site 882; the initiation of Northern Hemisphere glaciation, *Proc. Ocean Drill. Program Sci. Results*, *145*, 315–329.

Maslin, M. A., G. H. Haug, M. Sarnthein, and R. Tiedemann (1996), The progressive intensification of Northern Hemisphere glaciation as seen from the North Pacific, *Geol. Rundsch.*, *85*(3), 452–465, doi:10.1007/BF02369002.

Matsumoto, K., J. L. Sarmiento, and M. A. Brzezinski (2002), Silicic acid leakage from the Southern Ocean: A possible explanation for glacial atmospheric pCO_2, *Global Biogeochem. Cycles*, *16*(3), 1031, doi:10.1029/2001GB001442.

Mohan, R., S. Shanvas, M. Thamban, and M. Sudhakar (2006), Spatial distribution of diatoms in surface sediments from the Indian sector of Southern Ocean, *Curr. Sci.*, *91*(11), 1495–1502.

Murphy, L., D. A. Warnke, C. Andersson, J. Channell, and J. Stoner (2002), History of ice rafting at South Atlantic ODP Site 177–1092 during the Gauss and Late Gilbert Chrons, *Palaeogeogr. Palaeoclimatol. Palaeoecol.*, *182*(3–4), 183–196, doi:10.1016/S0031-0182(01)00495-3.

Ragueneau, O., et al. (2000), A review of the Si cycle in the modern ocean: Recent progress and missing gaps in the application of biogenic opal as a paleoproductivity proxy, *Global Planet. Change*, *26*(4), 317–365, doi:10.1016/S0921-8181(00)00052-7.

Raymo, M. E. (1994), The initiation of Northern Hemisphere glaciation, *Annu. Rev. Earth Planet. Sci.*, *22*, 353–383, doi:10.1146/annurev.ea.22.050194.002033.

Rea, D. K., and H. Schrader (1985), Late Pliocene onset of glaciation: Ice-rafting and diatom stratigraphy of North Pacific DSDP cores, *Palaeogeogr. Palaeoclimatol. Palaeoecol.*, *49*(3–4), 313–325, doi:10.1016/0031-0182(85)90059-8.

Rea, D. K., and H. Snoeckx (1995), Sediment fluxes in the Gulf of Alaska; paleoceanographic record from Site 887 on the Patton-Murray Seamount Platform, *Proc. Ocean Drill. Program Sci. Results*, *145*, 247–256.

Rea, D. K., et al. (1993), Site 882, *Proc. Ocean Drill. Program Initial Rep.*, *145*, 85–102.

Rea, D. K., H. Snoeckx, and L. H. Joseph (1998), Late Cenozoic eolian deposition in the North Pacific: Asian drying, Tibetan uplift, and cooling of the northern hemisphere, *Paleoceanography*, *13*(3), 215–224, doi:10.1029/98PA00123.

Reynolds, B. C., M. Frank, and A. N. Halliday (2006a), Silicon isotope fractionation during nutrient utilization in the North Pacific, *Earth*

Planet. Sci. Lett., *244*(1–2), 431–443, doi:10.1016/j.epsl.2006.02.002.

Reynolds, B. C., R. B. Georg, F. Oberli, U. H. Wiechert, and A. N. Halliday (2006b), Reassessment of silicon isotope reference materials using high-resolution multi-collector ICP-MS, *J. Anal. At. Spectrom.*, *21*(3), 266–269, doi:10.1039/b515908c.

Sarmiento, J. L., N. Gruber, M. A. Brzezinski, and J. P. Dunne (2004), High-latitude controls of thermocline nutrients and low latitude biological productivity, *Nature*, *427*(6969), 56–60, doi:10.1038/nature02127.

Shackleton, N. J., et al. (1984), Oxygen isotope calibration of the onset of ice-rafting and history of glaciation in the North Atlantic region, *Science*, *307*, 620–623.

Shemesh, A., R. A. Mortlock, R. J. Smith, and P. N. Froelich (1988), Determination of Ge/Si in marine siliceous microfossils: Separation, cleaning and dissolution of diatoms and radiolaria, *Mar. Chem.*, *25*(4), 305–323, doi:10.1016/0304-4203(88)90113-2.

Shemesh, A., L. H. Burckle, and P. N. Froelich (1989), Dissolution and preservation of Antarctic diatoms and the effect on sediment thanatocoenoses, *Quat. Res.*, *31*(2), 288–308, doi:10.1016/0033-5894(89)90010-0.

Sigman, D. M., M. A. Altabet, D. C. McCorkle, R. Francois, and G. Fischer (1999), The $\delta^{15}N$ of nitrate in the Southern Ocean: Consumption of nitrate in surface waters, *Global Biogeochem. Cycles*, *13*(4), 1149–1166, doi:10.1029/1999GB900038.

Sigman, D. M., S. L. Jaccard, and G. H. Haug (2004), Polar ocean stratification in a cold climate, *Nature*, *428*(6978), 59–63, doi:10.1038/nature02357.

Snoeckx, H., D. K. Rea, C. E. Jones, and B. L. Ingram (1995), Eolian and silica deposition in the central North Pacific: Results from sites 885/886, *Proc. Ocean Drill. Program Sci. Results*, *145*, 219–230.

Swann, G. E. A., M. A. Maslin, M. J. Leng, H. J. Sloane, and G. H. Haug (2006), Diatom $\delta^{18}O$ evidence for the development of the modern halocline system in the subarctic northwest Pacific at the onset of major Northern Hemisphere glaciation, *Paleoceanography*, *21*, PA1009, doi:10.1029/2005PA001147.

Talley, L. D., and T. M. Joyce (1992), The double silica maximum in the North Pacific, *J. Geophys. Res.*, *97*(C4), 5465–5480, doi:10.1029/92JC00037.

Tiedemann, R., and G. H. Haug (1995), Astronomical calibration of cycle stratigraphy for Site 882 in the northwest Pacific, *Proc. Ocean Drill. Program Sci. Results*, *145*, 283–292.

Tieszen, L. L. (1978), Carbon isotope fractionation in biological material, *Nature*, *276*(5683), 97–98, doi:10.1038/276097c0.

Treguer, P., D. M. Nelson, A. J. Vanbennekom, D. J. Demaster, A. Leynaert, and B. Queguiner (1995), The silica balance in the world ocean: A reestimate, *Science*, *268*(5209), 375–379, doi:10.1126/science.268.5209.375.

Tsuda, A., H. Saito, J. Nishioka, and T. Ono (2005), Mesozooplankton responses to iron-fertilization in the western subarctic Pacific (SEEDS2001), *Prog. Oceanogr.*, *64*(2–4), 237–251, doi:10.1016/j.pocean.2005.02.011.

Varela, D. E., C. J. Pride, and M. A. Brzezinski (2004), Biological fractionation of silicon isotopes in Southern Ocean surface waters, *Global Biogeochem. Cycles*, *18*, GB1047, doi:10.1029/2003GB002140.

Warren, B. A. (1983), Why is no deep water formed in the North Pacific, *J. Mar. Res.*, *41*(2), 327–347.

———————————

M. Frank, Leibniz Institute of Marine Sciences, at University of Kiel (IFM-GEOMAR), Wischhofstrasse 1-3, D-24148 Kiel, Germany.

A. N. Halliday, Department of Earth Sciences, Oxford University, South Parks Road, Oxford OX1 3PR, UK.

B. C. Reynolds, Institute of Isotope Geochemistry and Mineral Resources, ETH Zurich, CH-8092 Zurich, Switzerland. (reynolds@erdw.ethz.ch)